1 *Article*

2 # Optimum Design of Curved Surface Sliders for

3 # Minimum Structural Acceleration and Its Sensitivity

4 **Felix Weber [1],*, Leopold Meier [2], Johann Distl [3] and Christian Braun [4]**

5 [1] Maurer Switzerland GmbH, Neptunstrasse 25, 8032 Zurich, Switzerland; F.Weber@maurer.eu
6 [2] MAURER ENGINEERING GmbH, Frankfurter Ring 193, 80807 Munich, Germany; L.Meier@maurer.eu
7 [3] MAURER ENGINEERING GmbH, Frankfurter Ring 193, 80807 Munich, Germany; J.Distl@maurer.eu
8 [4] MAURER SE, Frankfurter Ring 193, 80807 Munich, Germany; C.Braun@maurer.eu
9
10 * Correspondence: F.Weber@maurer.eu; Tel.: +41-(0)44-520-8069
11

12 **Abstract:** The design of curved surface sliders (CSS) based on the elastic response spectrum is done
13 by iteration to find the combination of friction coefficient and displacement capacity which satisfies
14 the condition that the maximum horizontal CSS force is equal to the horizontal force of the
15 structure. Although this CSS design is valid it does not necessarily minimize structural
16 acceleration. This paper therefore describes the optimum CSS design for minimum structural
17 acceleration. All valid CSS designs and the optimum CSS design are represented by their associated
18 trajectory in the elastic response spectrum plane which visualizes the optimization problem. The
19 results demonstrate that the optimum CSS design is not obtained at maximum tolerated effective
20 damping ratio. The subsequent sensitivity analysis describes how much the structural acceleration
21 increases if the actual friction coefficient of the real CSS deviates from its optimum design value.
22 The analysis points out that the increase in structural acceleration is approximately one order of
23 magnitude smaller than the deviation in friction. The sensitivity data may be used by structural
24 engineer to determine tolerable deviations in friction coefficient which still results in acceptable
25 structural accelerations.

26 **Keywords:** curved surface slider; elastic response spectrum; friction; optimization; sensitivity
27

28 **1. Introduction**

29   Curved surface sliders (CSS) shift the natural period of the primary structure away from the
30 time period range of high seismic energy and augment structural damping by friction damping [1].
31 For a selected isolation time period the CSS may be designed by the elastic response spectrum
32 method assuming friction coefficient and displacement capacity [2]. A valid CSS design is obtained if
33 the maximum longitudinal CSS force is equal to the maximum horizontal force of the primary
34 structure due to the ground acceleration [2]. Thus, infinite CSS designs may be obtained by different
35 combinations of friction coefficient and displacement capacity but there is only one combination
36 minimizing structural acceleration. This design freedom led to a variety of investigations on the
37 damping in CSS. Back in 1991 Lai and Song [3] started investigating the impact of CSS damping on
38 structural acceleration, followed by Inaudi and Kelly [4] in 1993. Later the controversy discussion on
39 the role of linearized CSS damping on CSS displacement capacity and structural acceleration was
40 published in 1999 by Kelly [5] and Hall [6]. Du and Zhaou [7] used a linearized 2-degree-of-freedom
41 model of the structure with CSS to investigate the optimum damping range of CSS. A first approach
42 towards the optimization of the friction coefficient of CSS was presented by Jangid [8] in 2005 where
43 the optimization criterion was to minimize both top floor acceleration and CSS relative motion for
44 near-fault motion. Depending on the ground motion data the optimum friction coefficients turned
45 out to be between 5% and 15%. Bucher [9] extended this optimization task by also taking into
46 consideration the re-centring condition and Kovaleva et al. [10] further developed this approach to

47 derive optimum CSS parameters for various optimization functions. In the work of Nigdeli et al. [11]
48 a linearized model of the structure with CSS was adopted to derive optimum CSS parameters that
49 minimize structural acceleration with the constraint of a maximum tolerated CSS displacement
50 capacity; a similar approach was used by Kamalzare et al. [12] to keep computational efforts within
51 reasonable limits.

52   Common to most of the above mentioned studies is that basically optimum results only are
53 shown but not all valid CSS design solutions. Also, the results of these studies are valid for certain
54 ground motion data but not for the entire possible variety of ground accelerations as specified by the
55 elastic response spectra of type 1 and 2 with soil classes A, B, C, D and E [2]. This paper tries to fill
56 this gap by first showing the characteristics of all valid CSS designs from which the optimum CSS
57 design for minimum structural acceleration directly follows. In a next step it is shown how the
58 characteristic variables such as friction coefficient, displacement capacity, effective damping ratio,
59 reduction factor, effective time period and re-centring condition of all optimum CSS solutions
60 depend on the selection of the isolation time period. These two first studies are performed for
61 spectra of type 1 and 2 and soil class C. In the third and final section of the paper a sensitivity study
62 is presented for all spectra types and soil classes which describes by how much structural
63 acceleration will deteriorate when the actual friction coefficient of the real CSS differs from its
64 optimum value. This study gives a clear statement on the acceptable tolerance of the friction
65 coefficient of CSS and can be used by structural engineers to determine maximum tolerable
66 deviations in the actual friction coefficient to still guarantee acceptably small structural
67 accelerations.

2. Optimum Curved Surface Sliders for minimum structural acceleration

69   Section 2.1 describes the CSS design adopting the linear elastic response spectrum method. The
70 graphical representation of all valid CSS designs in the response spectrum plane is shown and
71 discussed in section 2.2 based on which the optimization routine is presented to obtain the optimum
72 CSS design for minimum structural acceleration response. The optimization results for spectra of
73 type 1 and 2 are given in sections 2.3 and 2.4.

74 *2.1. Linear elastic response spectrum method*

75   The linear response spectrum describes the peak acceleration S_e normalized by the peak
76 ground acceleration a_g as function of the time period T of the structure modelled as single
77 degree-of-freedom (DOF) system whose damping ratio ζ_S is 5% (Figure 1) [2]. The spectra of
78 different earthquakes and soil classes are defined by their peak ground acceleration a_g, their type
79 (1 or 2), their soil parameter S and time periods T_B, T_C and T_D. The acceleration response at
80 time periods $T_B \leq T < T_C$ is constant, at $T_C \leq T < T_D$ in proportion to T^{-1} whereby its velocity is
81 constant and at $T_C \leq T < T_D$ in proportion to T^{-2} which results in constant displacement.

82   Once the spectrum is defined by the soil dynamics experts the CSS design starts by the selection
83 of the targeted isolation time period T_{iso} of the structure with CSS which determines the effective
84 radius R_{eff} of the curved surface of the CSS according to $R_{eff} = g(T_{iso}/2/\pi)^2$. Then, a
85 combination of friction coefficient μ and displacement capacity d_{bd} of the CSS must be assumed
86 in order to be able to compute the following states (Figure 2):

87 - maximum horizontal CSS force: $F_b = \mu N_S + d_{bd} \dfrac{N_S}{R_{eff}}$ \hfill (1)

88 - effective stiffness: $k_{eff} = \dfrac{F_b}{d_{bd}}$ (not equal to restoring stiffness N_S/R_{eff}) \hfill (2)

89 - effective time period: $T_{eff} = 2\pi \sqrt{\dfrac{N_S}{g\,k_{eff}}}$ \hfill (3)

90   • effective damping ratio: $\zeta_{\text{eff}} = \dfrac{2\mu}{\pi\left(\mu + \dfrac{d_{bd}}{R_{\text{eff}}}\right)}$ with constraint $\zeta_{\text{eff}} \leq 30\%$ (4)

91   • reduction factor: $\eta = \sqrt{\dfrac{0.10}{0.05 + \zeta_{\text{eff}}}}$ with constraints $0.55 \leq \eta \leq 1$ (5)

92   • reduced acceleration response of structure at effective time period: $\eta S_e (T = T_{\text{eff}})$ (6)
93   (acceleration response determined from spectrum and multiplied by η)

94   • maximum horizontal force of structure (single DOF): $F_S = \eta S_e \dfrac{N_S}{g}$ (7)

95   where N_S denotes the vertical load in Newton on the CSS, g =9.81 m/s² is the gravitational field
96   constant, ζ_{eff} must not be greater than 30% for linear calculation, the reduction factor η is limited
97   to 1 if $\zeta_{\text{eff}} \leq \zeta_S$ =5% and $\eta \geq 0.55$ limits the reduction of the acceleration response of the structure if
98   $\zeta_{\text{eff}} > 5\%$. Solving (5) for ζ_{eff} with η =0.55 yields ζ_{eff} =28.1% (approx.) which shows that the
99   minimum tolerated reduction factor η=0.55 is triggered by ζ_{eff} being smaller than its maximum
100 tolerated value of 30% for linear calculation.
101   A valid CSS design is obtained if the maximum horizontal force (1) of the CSS is equal to the
102 maximum horizontal force (7) of the structure (with a reasonable error tolerance). If this condition is
103 not fulfilled the values assumed for μ and d_{bd} must be altered until $F_b \approx F_S$ is obtained. As the
104 primary goal of this iterative procedure, which is commonly made by trial and error, is to satisfy
105 $F_b \approx F_S$ the resulting CSS design – although a valid design – does not necessarily also minimize the
106 acceleration response of the structural. The subsequent section therefore describes a procedure how
107 to obtain all valid CSS designs due to all possible combinations of μ and d_{bd} based on which the
108 CSS design leading to minimum structural acceleration can be identified.
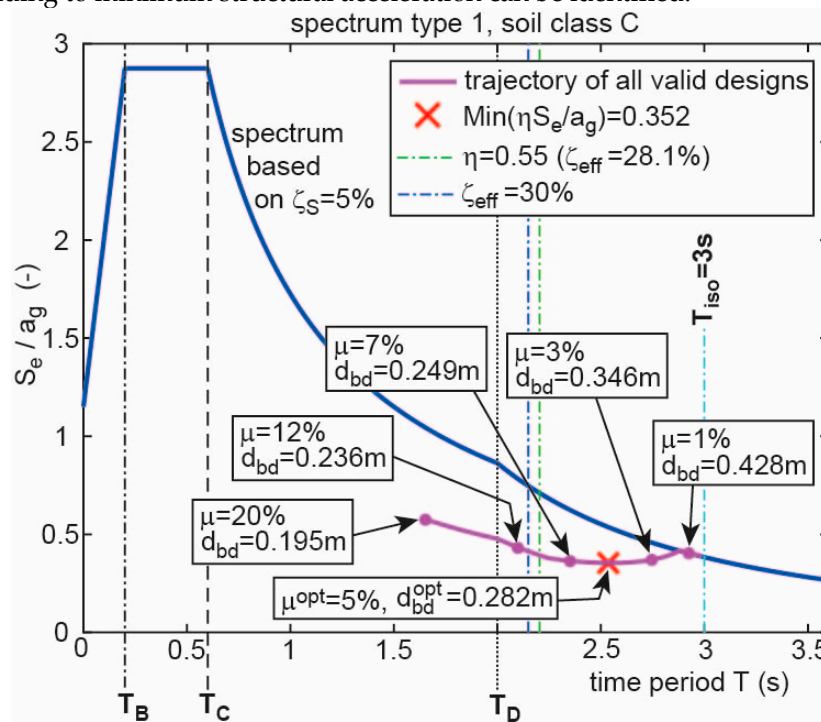
109

110   **Figure 1.** Elastic response spectrum including trajectory of all valid CSS designs, limitations due to
111   minimum reduction factor and maximum effective damping ratio and optimum CSS design for minimum
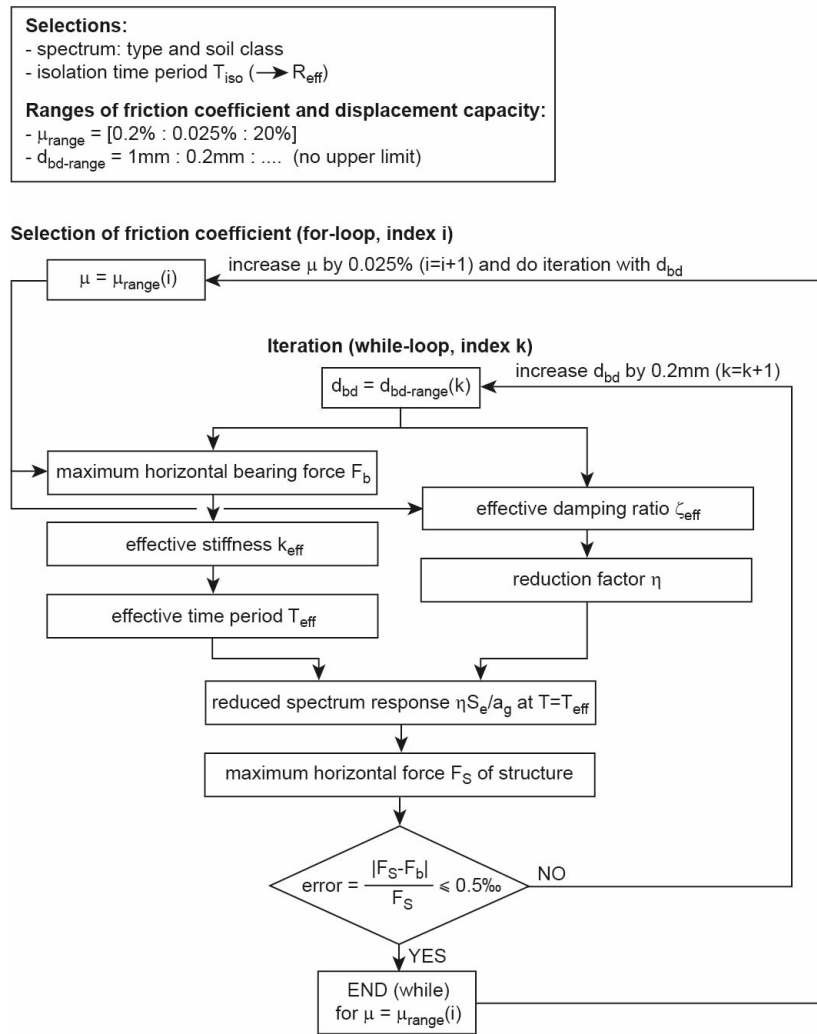112   structural acceleration.

Figure 2. Flow chart of software program to compute all valid CSS designs.

2.2. Optimum CSS design for minimum structural acceleration

A software program is presented which allows computing any valid CSS design based on different combinations of μ and d_{bd} satisfying $F_b \approx F_S$; Figure 2 depicts the flow chart of this software program. The software program basically consists of a for-loop where μ is selected based on the assumed friction coefficient range μ_{range} beginning at $\mu = 0.2\%$ and ending at $\mu = 20\%$ with increment of 0.025% and a while-loop that computes d_{bd} for the selected μ such that the relative error of $F_b \approx F_S$ is not greater than 0.5‰. For the assumed friction coefficient range with 792 elements this software program computes 792 valid CSS designs. These valid CSS designs are plotted in the spectrum plane in Figure 1 by their reduced normalized structural acceleration response $\eta\, S_e / a_g$ versus their effective time period T_{eff}. Due to the small increment in μ_{range} the plotted points of these valid CSS designs appear as a line, i.e. the **trajectory of valid CSS designs**. Along this trajectory the design parameters μ and d_{bd} of the valid CSS designs change which is shown by some selected valid CSS designs with associated values of μ and d_{bd}. From this trajectory the following can be observed:

a) The trajectory of the valid CSS designs starts at $T_{eff} \approx T_{iso}$ due to the smallest considered friction coefficient $\mu = 0.2\%$ and then primarily propagates to the "left", i.e. to lower values of T_{eff} due to the increasing values of μ and the acceleration response of the trajectory is reduced due to $0.55 \leq \eta \leq 1$.

133   b)   As long as $\zeta_{\text{eff}} \leq 5\%$ the trajectory of the valid CSS designs is congruent with the non-reduced
134   acceleration response of the spectrum because $\zeta_{\text{eff}} \leq \zeta_S = 5\%$ leads to $\eta = 1$.
135   c)   For $5\% < \zeta_{\text{eff}} \leq 28.1\%$ the trajectory of the valid CSS designs is below the non-reduced
136   acceleration response of the spectrum because $5\% < \zeta_{\text{eff}} \leq 28.1\%$ results in $0.55 \leq \eta < 1$.
137   d)   To the "left" of the vertical dash-dotted line in green due to $\zeta_{\text{eff}} = 28.1\%$ and hence $\eta = 0.55$
138   the reduction factor remains at 0.55 despite ζ_{eff} increases up to its maximum tolerated value
139   of 30% due to the increasing μ; $\zeta_{\text{eff}} = 30\%$ is indicated by the blue vertical dash-dotted line.
140   e)   **There exists one optimum CSS design that is valid (** $F_b \approx F_S$ **) and minimizes the structural**
141   **acceleration response** which is highlighted by the red cross on the trajectory.
142   The optimum CSS design is determined by the described software program after the computation of
143   all valid CSS designs from which the pair of μ and d_{bd} is selected that minimizes the structural
144   acceleration response. In the subsequent section 2.3 and 2.4 the optimum CSS designs are presented
145   for spectra of type 1 and 2 and soil class C; the results due to other soil classes are omitted as their
146   influence on the optimization results is little.

147   *2.3. Optimization results for spectrum of type 1 with soil class C*

148   2.3.1. Optimum solutions for selected isolation time periods

149   Four optimization trajectories due to four selected isolation time periods are presented.
150   Figure 3(a) depicts the case of a rather unrealistically low isolation time period $T_{\text{iso}} = 1.9$ s whereby
151   the entire optimization trajectory lies in the region $T_C \leq T_{\text{eff}} < T_D$. The optimum CSS design is
152   obtained at minimum tolerated $\eta = 0.55$ due to $\zeta_{\text{eff}} = 28.1\%$, i.e. on the green dash-dotted line. For the
153   more realistic isolation time period $T_{\text{iso}} = 3.5$ s the main part of the optimization trajectory including
154   the optimum CSS design lies in the region $T_{\text{eff}} \geq T_D$ (Figure 3(b)). The optimum CSS design is
155   characterized by $\zeta_{\text{eff}} = 17.8\%$ and $\eta = 0.662$. The optimization trajectory does not show how the state
156   variables μ, d_{bd}, ζ_{eff}, η and T_{eff} change along the trajectory. Therefore, the state variables
157   d_{bd}, ζ_{eff}, η and T_{eff} are plotted as function of the varied μ in Figures 4 and 5 for $T_{\text{iso}} = 1.9$ s
158   and $T_{\text{iso}} = 3.5$ s. The force displacement loop of the optimum CSS solution is also included to
159   demonstrate that the optimum CSS design fulfils the re-centring condition $E_s / E_h \geq 0.25$.
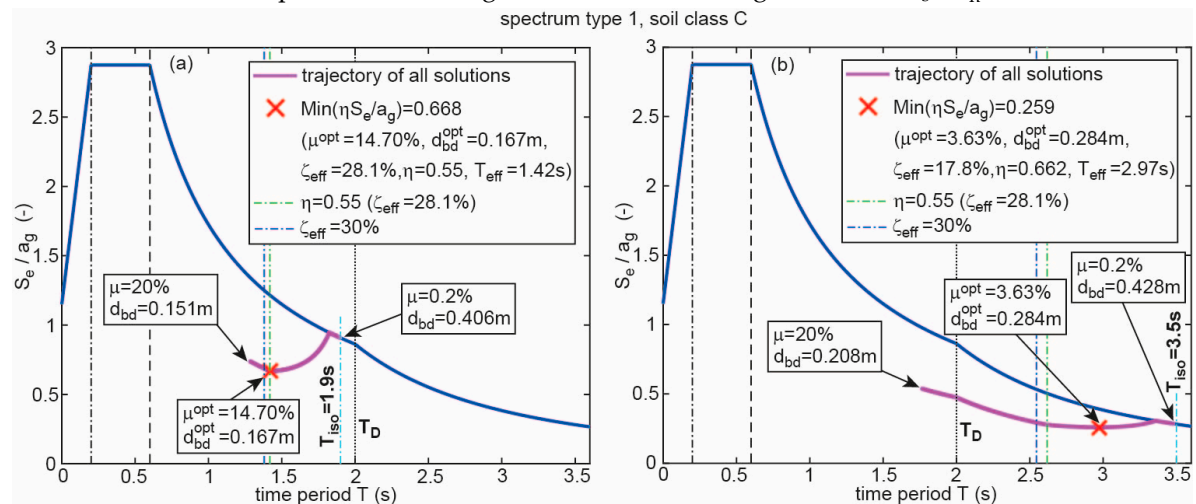

160

161   **Figure 3.** Optimization trajectories for (**a**) $T_{\text{iso}} = 1.9$ s and (**b**) $T_{\text{iso}} = 3.5$ s for spectrum type 1 with soil
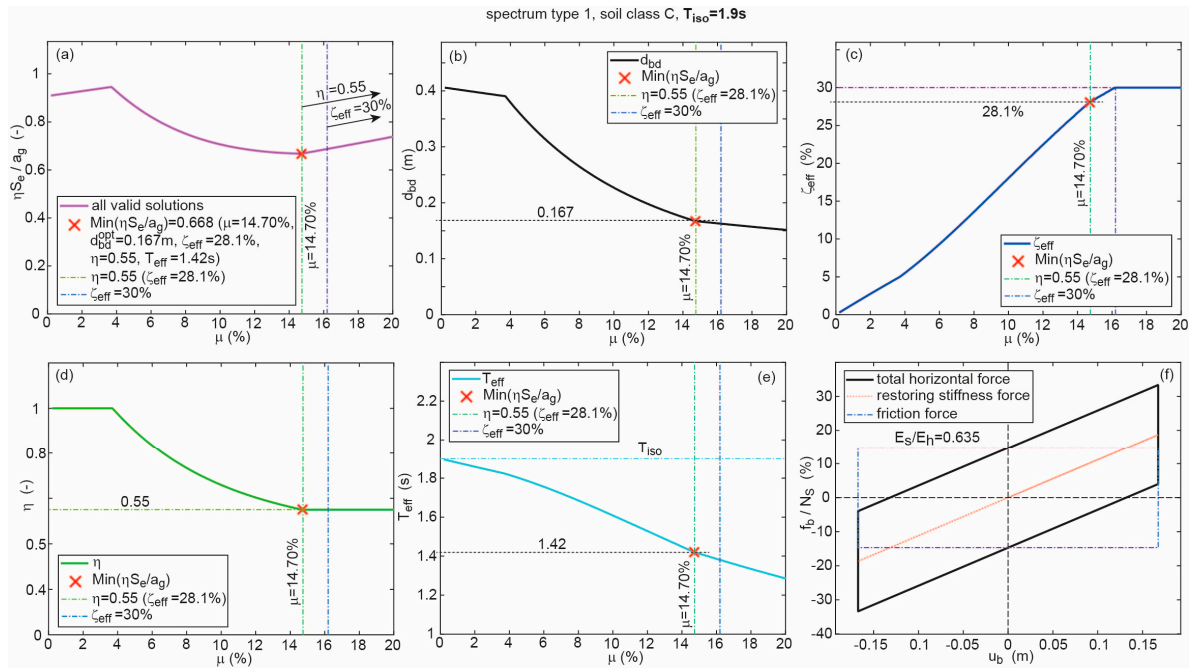162   class C.

Figure 4. (**a-e**) Optimization results for T_{iso} =1.9 s as function of friction coefficient and (**f**) force displacement curve of optimum CSS design for spectrum type 1 with soil class C.
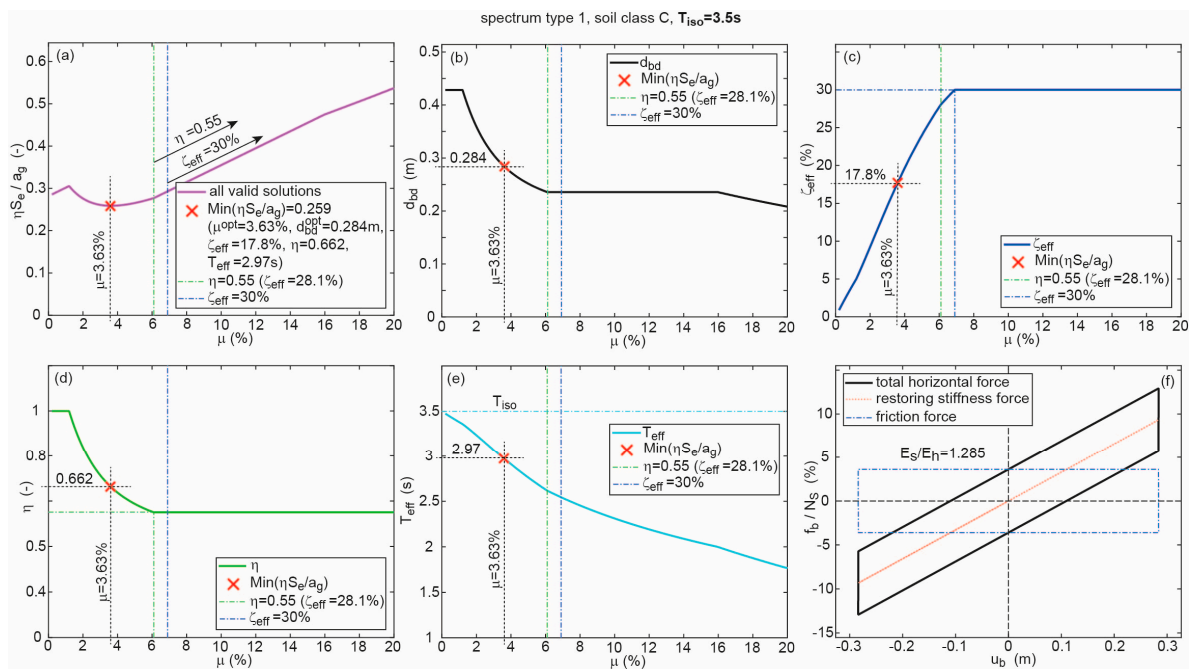

Figure 5. (**a-e**) Optimization results for T_{iso} =3.5 s as function of friction coefficient and (**f**) force displacement curve of optimum CSS design for spectrum type 1 with soil class C.

The location of the optimum CSS design becomes nontrivial when the optimizations are performed for T_{iso} =1.49 s (Figure 6) and T_{iso} =1.50 s (Figure 7). For T_{iso} =1.49 s the optimum CSS design lies in the region $T_{eff} < T_D$ because the optimization trajectory, which shows a first local minimum at $T_{eff} > T_D$ in section (ii), drops again in section (iii) generating the **global minimum** at $T_{eff} < T_D$ (Figure 6(b)). The optimum CSS design is characterized by ζ_{eff} =28.1% and η =0.55. In contrast, if T_{iso} =1.50 s is selected the global minimum is obtained at $T_{eff} > T_D$ with ζ_{eff} =17.8% and η =0.662 similar to the results obtained for T_{iso} =3.50 s (Figure 7(b)).
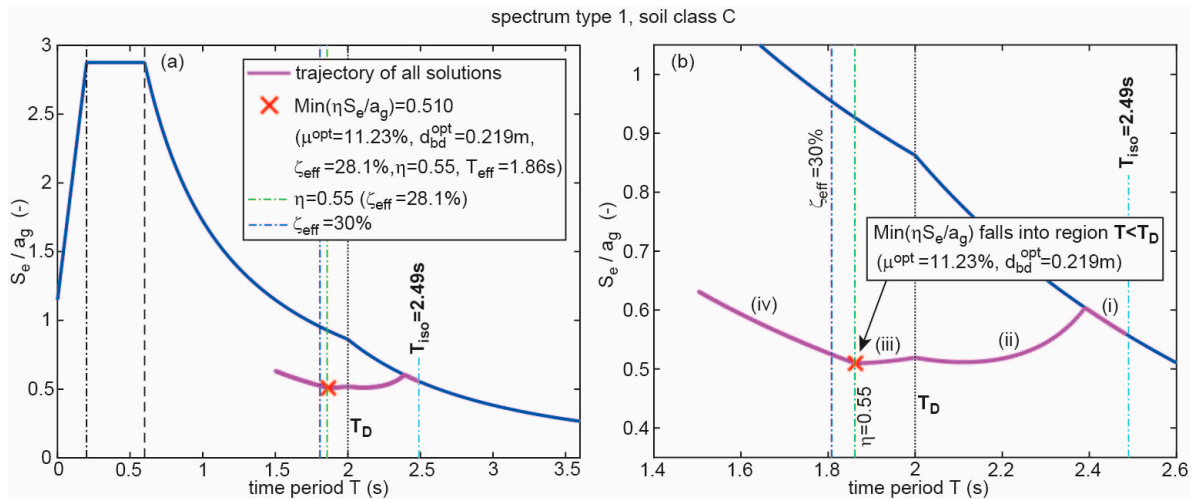
Figure 6. (**a**) Optimization trajectory for T_{iso} =2.49 s and (**b**) according close-up for spectrum type 1 with soil class C.
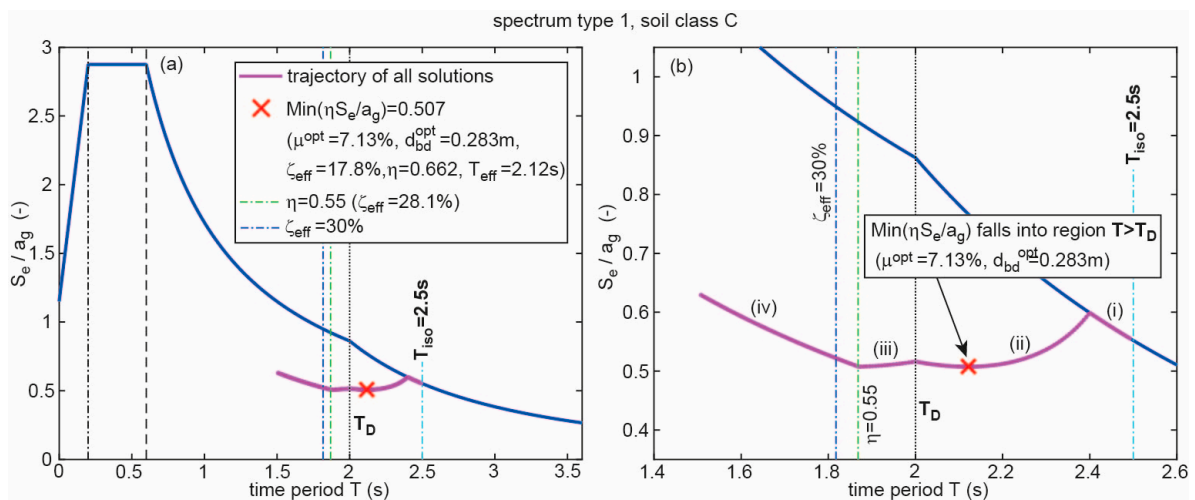

Figure 7. (**a**) Optimization trajectory for T_{iso} =2.5 s and (**b**) according close-up for spectrum type 1 with soil class C.

2.3.2. Optimum solutions as function of isolation time period

In section 2.3.1 the optimization trajectories with the according optimum CSS designs are shown for some selected isolation time periods, i.e. T_{iso} =1.9 s, 2.49 s, 2.5 s and 3.5 s. The logical next step is to have a look only at how the optimum CSS design solutions depend on T_{iso}. Figure 8 shows how the optimum design parameters of the CSS, i.e. the optimum friction coefficient μ^{opt} and the optimum displacement capacity d_{bd}^{opt}, and the resulting minimized structural acceleration response depend on T_{iso}. The other state variables of interest of the optimum CSS design solutions, i.e. ζ_{eff}, η, T_{eff}, F_b / N_S and E_s / E_h, are depicted in Figure 9 as function of T_{iso}. The following main observation can be made:

- The **longer** T_{iso} is the **smaller the optimum friction coefficient** μ^{opt} becomes.
- The **displacement capacities** d_{bd}^{opt} **of all optimum CSS design solutions** whose effective time periods lie in the region $T_{eff} > T_D$ **are constant** because at $T_{eff} > T_D$ the reduction factor η =0.66 is constant and $\eta S_e / a_g$ at $T_{eff} > T_D$ is in proportion to $1/T^2$ whereby the according displacement is constant.; notice that d_{bd}^{opt} =constant at $T_{eff} > T_D$ only applies to the optimum CSS design solutions due to η =constant in this time period range.

- The **optimum CSS design** in the typical isolation time period region 3.5 s $< T_{iso} < 5$ s is **not obtained from maximum tolerated effective damping ratio** $\zeta_{eff} = 30\%$ but from the lower value $\zeta_{eff} = 17.8\%$ evoking $\eta = 0.66$.

- The jump in the curves of the shown state variables at $T_{iso} = 2.5$ s is caused by the fact that the optimum CSS design lies in the region $T_{eff} < T_D$ if $T_{iso} < 2.5$ s while it is located in the region $T_{eff} > T_D$ if $T_{iso} \geq 2.5$ s.

- Reasonable values for F_b / N_S are found in the typical isolation time period region 3.5 s $< T_{iso} < 4.5$ s.

- The re-centring condition $E_s / E_h \geq 0.25$ is fulfilled for all optimum CSS design solutions for all considered T_{iso}.
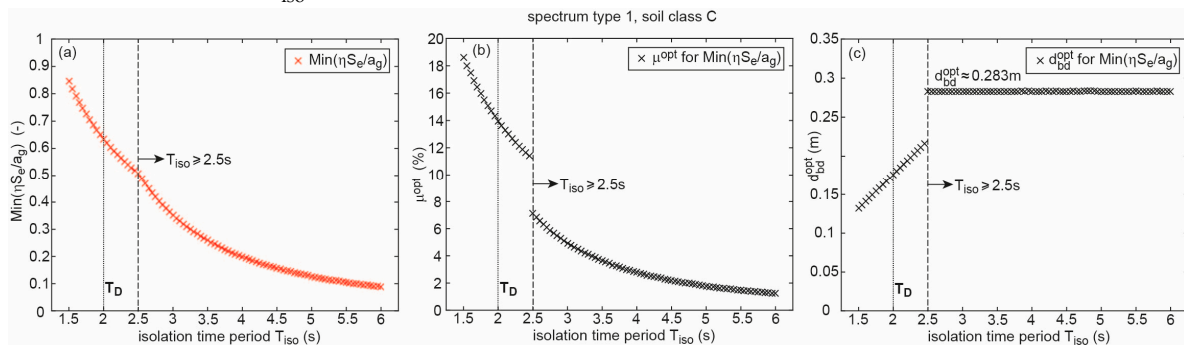

Figure 8. (**a**) Minimum structural acceleration due to optimum selections of (**b**) friction coefficient and (**c**) displacement capacity for spectrum type 1 with soil class C.
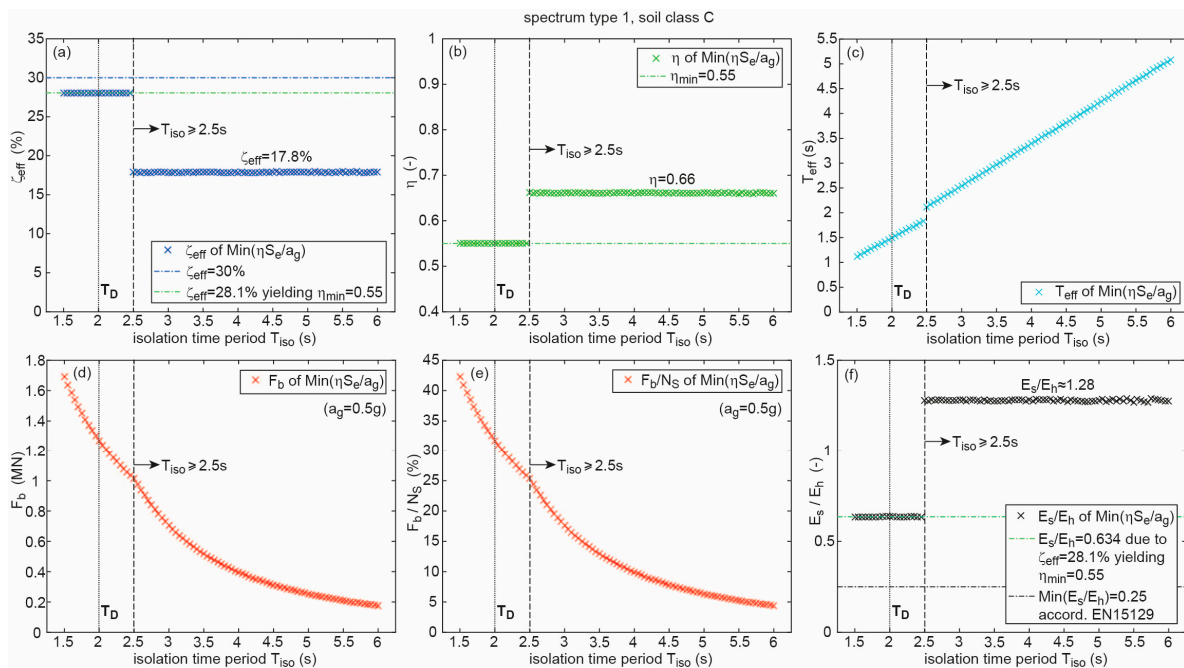

Figure 9. States of optimum solution: (**a**) effective damping ratio, (**b**) reduction factor, (**c**) effective time period, (d, e) maximum horizontal CSS force, (f) re-centring condition for spectrum type 1 with soil class C.

2.4. Optimization results for spectrum of type 2 with soil class C

The optimization trajectories associated by their optimum CSS designs for spectrum type 2 and soil class C are depicted in Figures 10 and 11. Since $T_D = 1.2$ s for type 2 is much lower than $T_D = 2$ s for type 1 the optimum CSS design solution lies in the region $T_{eff} < T_D$ if $T_{iso} < 1.5$ s and in $T_{eff} > T_D$

218   if $T_{iso} \geq 1.5$ s which explains the jump in the state variables at T_{iso} =1.5 s (Figures 12 and 13). Similar

219   to the results for spectrum of type 1 not the maximum tolerated effective damping ratio ζ_{eff} =30%

220   with associated η =0.55 but ζ_{eff} =17.6% with associated η =0.66 minimizes structural acceleration.

221   Also, the re-centring condition is fulfilled for all considered T_{iso} and shows the same value as for
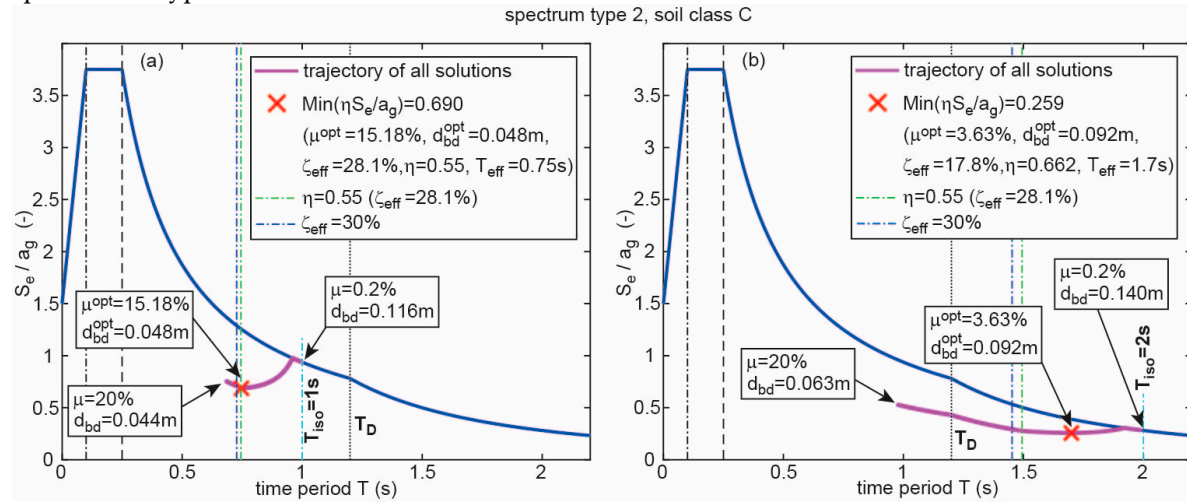
222   spectrum of type 1.

223

224   **Figure 10.** Optimization trajectories for (**a**) T_{iso} =1 s and (**b**) T_{iso} =2 s for spectrum type 2 with soil class C.

225

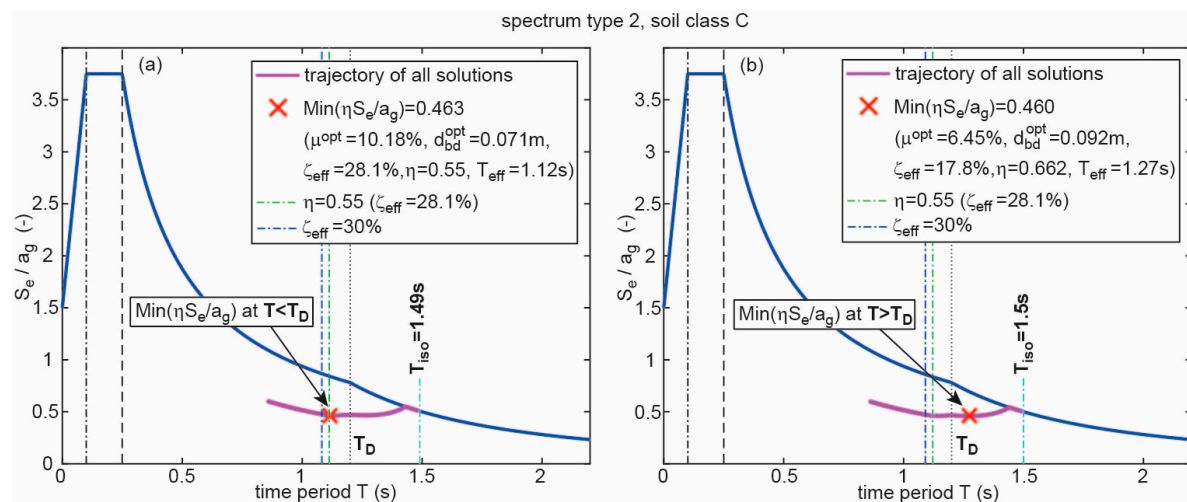226   **Figure 11.** Optimization trajectories for (**a**) T_{iso} =1.49 s and (**b**) T_{iso} =1.5 s for spectrum type 2 with soil

227   class C.
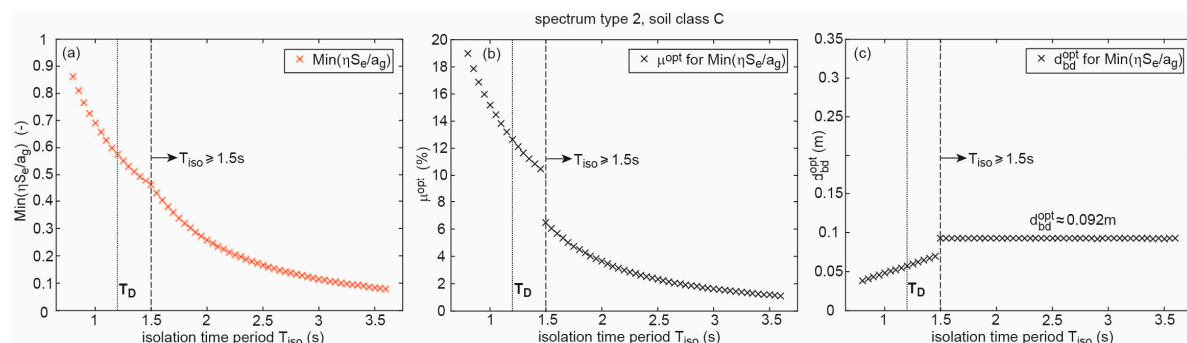

228

229   **Figure 12.** (**a**) Minimum structural acceleration due to optimum selections of (**b**) friction coefficient and (**c**)
230   displacement capacity for spectrum type 2 with soil class C.
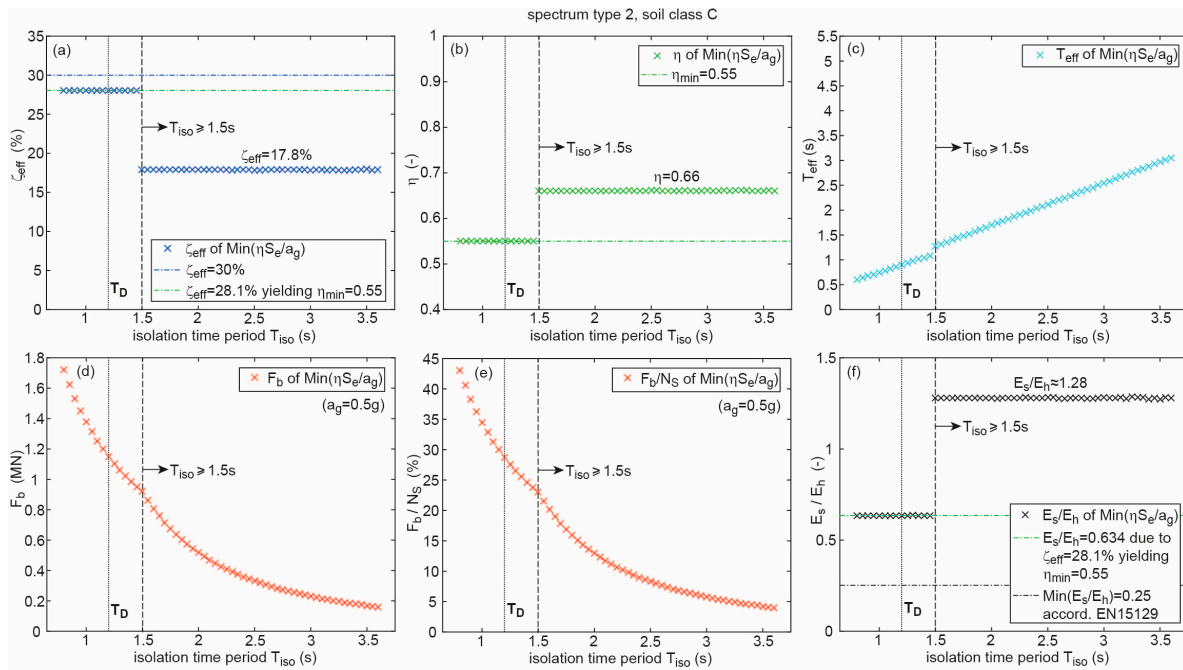
Figure 13. States of optimum solution: (**a**) effective damping ratio, (**b**) reduction factor, (**c**) effective time period, (d, e) maximum horizontal CSS force, (f) re-centring condition for spectrum type 2 with soil class C.
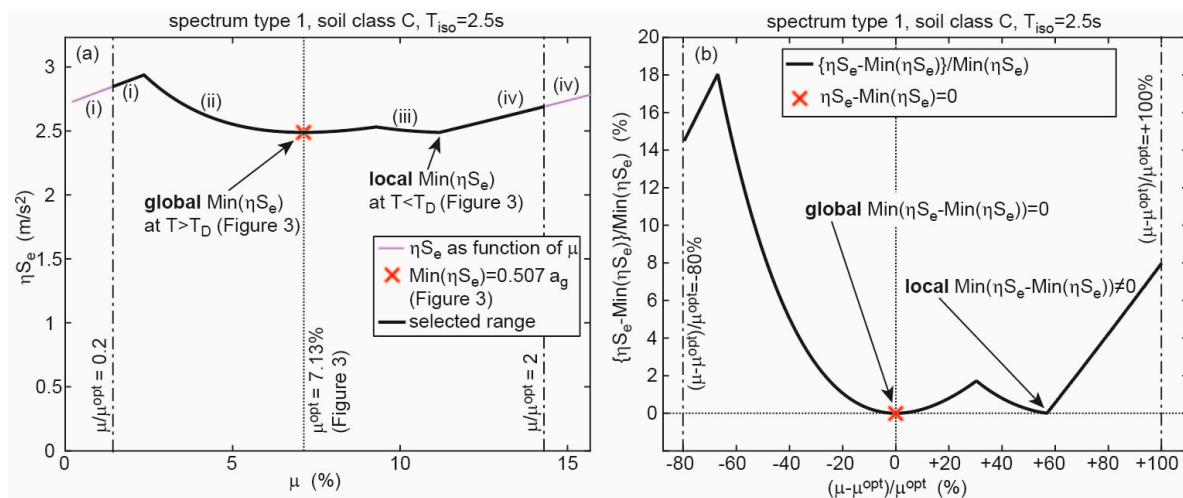

Figure 14. Derivation of sensitivity curves (shown for spectrum type 1 with soil class C and T_{iso} =2.5 s): (**a**) reduced acceleration response ηS_e as function of friction coefficient μ and (**b**) according sensitivity curve.

3. Sensitivity of friction coefficient on structural acceleration

This section describes quantitatively by how much the structural acceleration worsens when the actual friction coefficient of the real CSS deviates from its optimum value minimizing structural acceleration.

3.1. Sensitivity formulation

The reduced structural acceleration response ηS_e computed as function of friction coefficient μ as depicted in Figure 14(a) basically shows by how much the structural acceleration response deteriorates (increases) if the actual friction coefficient of the real CSS deviates (being smaller or greater) from its optimum value μ^{opt}. The sensitivity is defined as the relative change in the

248　system's output (relative change in structural acceleration) for given relative change in the system's
249　input (relative change in friction coefficient). Hence, the sensitivity curve is obtained by, first,
250　subtracting the minimum value from the structural acceleration and the optimum value from the
251　friction coefficient, respectively, and, subsequently, normalizing the first term by its minimum value
252　and the second term by its optimum value (Figure 14(b))

253
$$\text{sensitivity} = \frac{\{\eta S_e - \text{Min}(\eta S_e)\}/\text{Min}(\eta S_e)}{\{\mu - \mu^{opt}\}/\mu^{opt}} = \frac{\delta S_e / S_e^{opt}}{\delta \mu / \mu^{opt}} \tag{8}$$

254　　　　Please note that this sensitivity analysis does not investigate the impact of deviations in μ on
255　the resulting displacement capacity. It is common understanding that a lower actual friction
256　coefficient of the real CSS than its design value will cause larger relative motions in the CSS as, e.g.,
257　visible in Figures 4(b) and 5(b).

258　*3.2. Results for spectrum of type 1*

259　　　　The sensitivity curves for spectrum of type 1 with soil class C are depicted in Figures 15-17 for
260　the selected isolation time periods T_{iso} =2 s, 2.5 s, 3 s, 3.5 s, 4 s and 4.5 s. The sensitivity curves for
261　the unusually low T_{iso} =2 s and 2.5 s are also plotted to demonstrate that structural acceleration is
262　more sensitive to deviations in the actual friction coefficient if T_{iso} is unusually low (2 s) and that
263　structural acceleration does hardly deteriorate for $\mu - \mu^{opt}$ >0 if T_{iso} =2.5 s due to the special case that
264　the global and local minima yield a fairly flat sensitivity curve at $\mu - \mu^{opt}$ >0. Horizontal dash-dotted
265　lines in different colours corresponding to different levels of deterioration in $\delta S_e / S_e^{opt}$ are included
266　in Figures 15-17 to be able to directly read off by how much the actual friction coefficient may
267　deviate (plus and minus) from its optimum value if a certain level of acceptable deterioration in
268　structural acceleration is assumed. For instance the structural engineer may estimate that the
269　structural acceleration may deteriorate by +5% (green dash-dotted line) and then read off directly
270　from the sensitivity curves by how much the actual friction coefficient of the real CSS may differ
271　from its optimum value. For the assumption that $\delta S_e / S_e^{opt}$ =+5% may be acceptable the sensitivity
272　curves with reasonable isolation time periods T_{iso} =3 s to 4.5 s demonstrate that the actual friction
273　coefficient of the real CSS may deviate from its optimum value by at least $\delta \mu / \mu^{opt}$ =-39.7% and
274　+55.6%. The tolerances are not symmetric relative to μ^{opt} because of the non-symmetrical
275　sensitivity curves.

276

278　**Figure 15.** Sensitivity of deviation in friction coefficient from its optimum value on relative increase of
279　structural acceleration for (**a**) T_{iso} =2 s and (**b**) T_{iso} =2.5 s and spectrum of type 1 with soil class C.
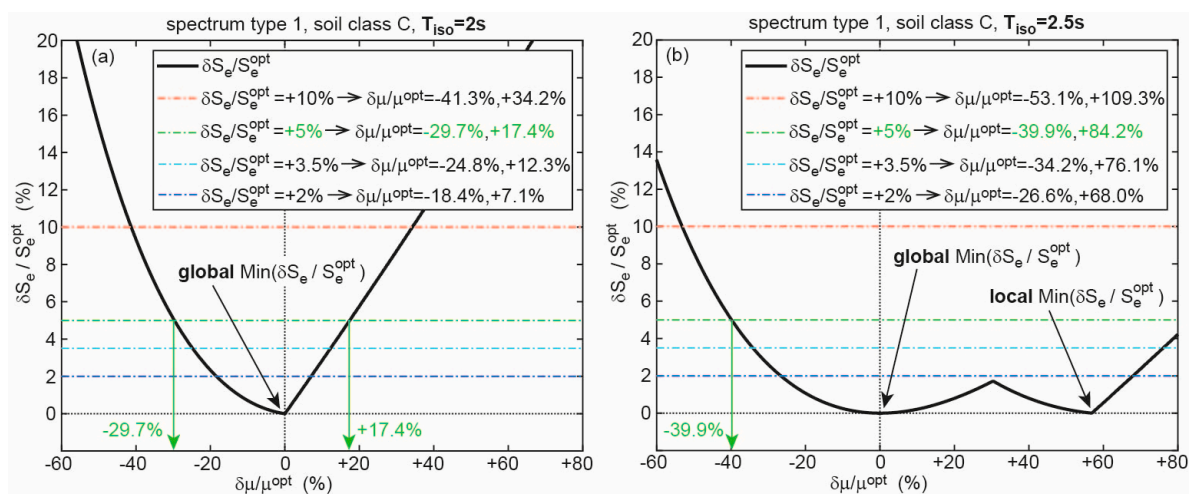
Figure 16. Sensitivity of deviation in friction coefficient from its optimum value on relative increase of structural acceleration for (**a**) T_{iso} =3 s and (**b**) T_{iso} =3.5 s and spectrum of type 1 with soil class C.
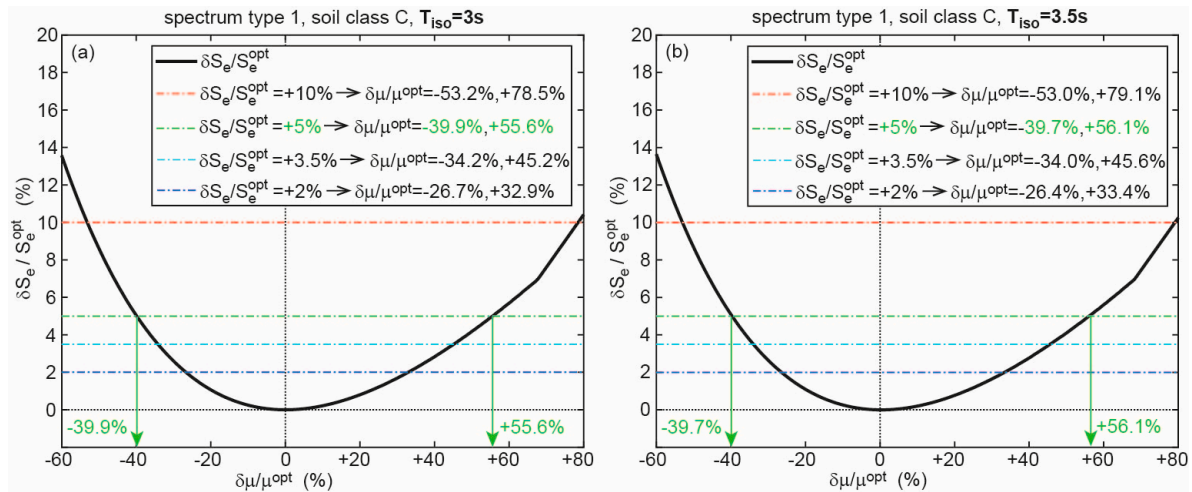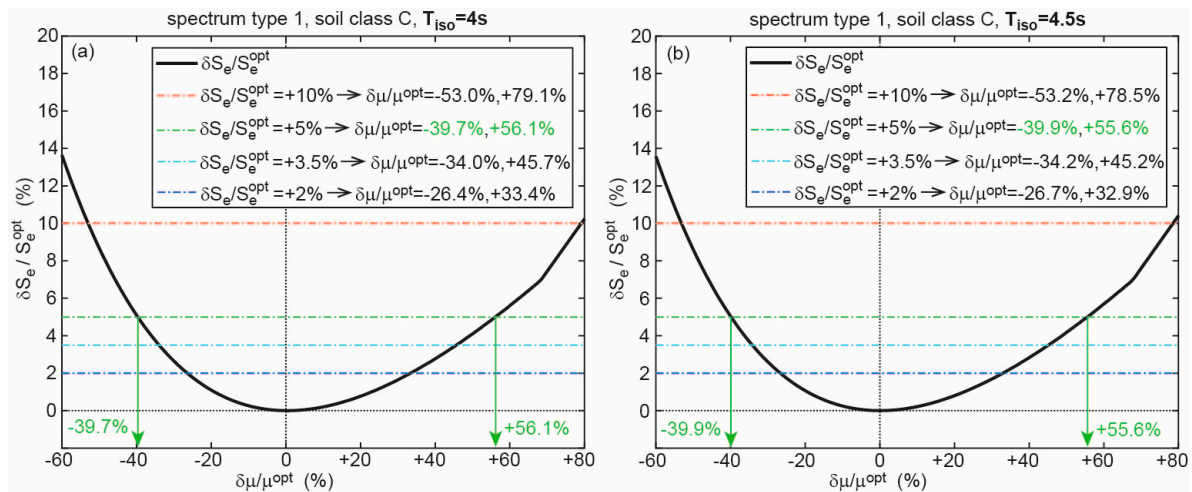

Figure 17. Sensitivity of deviation in friction coefficient from its optimum value on relative increase of structural acceleration for (**a**) T_{iso} =4 s and (**b**) T_{iso} =4.5 s and spectrum of type 1 with soil class C.

Sensitivity curves are also computed for spectrum of type 1 with soil classes A, B, D and E. The results of these computations are evaluated for acceptable deteriorations in $\delta S_e / S_e^{opt}$ of +5% and +2% and summarized in Table 1 together with the results for spectrum of type 1 with soil class C. This table reveals that – for reasonable isolation time periods $T_{iso} \geq 3$ s for spectrum of type 1 – the actual friction coefficient of the real CSS may differ from its optimum value by at least $\delta\mu / \mu^{opt}$ =-39.4% and +54.5% if $\delta S_e / S_e^{opt}$ =+5% may be acceptable and by at least $\delta\mu / \mu^{opt}$ =-26.4% and +32.5% if $\delta S_e / S_e^{opt}$ =+2% is considered to be acceptable.

3.3. Results for spectrum of type 2

Analogue to the results for spectrum of type 1 the sensitivity curves for spectrum of type 2 with soil class C are graphically presented (Figures 18-20) and all sensitivities resulting from spectrum of type 2 with all soil classes evaluated at $\delta S_e / S_e^{opt}$ =+5% and +2% are summarized in Table 2. For reasonable $T_{iso} \geq 1.8$ s it is seen that the actual friction coefficient of the real CSS may differ from its optimum value by at least $\delta\mu / \mu^{opt}$ =-39.7% and +54.5% assuming $\delta S_e / S_e^{opt}$ =+5% is acceptable and by at least $\delta\mu / \mu^{opt}$ =-26.4% and +32.0% if $\delta S_e / S_e^{opt}$ =+2% is assumed to be acceptable. These results

300 are very similar to those for spectrum of type 1 because the relative deterioration of the structural
301 acceleration depends on the relative change of the friction coefficient.

302 **Table 1.** Sensitivity results for spectrum of type 1 for relative increase of +5% and +2% in structural
303 acceleration.

T_{iso} (s)	soil class	$\delta S_e / S_e^{opt}$	$\delta\mu / \mu^{opt}$	$\delta S_e / S_e^{opt}$	$\delta\mu / \mu^{opt}$
2	A	+5%	-29.6%, +17.7%	2%	-18.3%, +7.3%
	B	+5%	-29.7%, +17.4%	2%	-18.4%, +7.0%
	C	+5%	-29.7%, +17.4%	2%	-18.4%, +7.1%
	D	+5%	-29.6%, +17.5%	2%	-18.3%, +7.1%
	E	+5%	-29.6%, +17.6%	2%	-18.3%, +7.2%
2.5	A	+5%	-39.8%, +84.4%	2%	-26.6%, +68.1%
	B	+5%	-39.9%, +84.0%	2%	-26.7%, +67.8%
	C	+5%	-39.9%, +84.2%	2%	-26.6%, +68.0%
	D	+5%	-39.9%, +84.1%	2%	-26.7%, +67.9%
	E	+5%	-39.9%, +84.2%	2%	-26.7%, +67.9%
3	A	+5%	-40.0%, +55.2%	2%	-26.9%, +32.7%
	B	+5%	-39.8%, +55.7%	2%	-26.6%, +33.0%
	C	+5%	-39.9%, +55.6%	2%	-26.7%, +32.9%
	D	+5%	-39.9%, +55.5%	2%	-26.7%, +32.8%
	E	+5%	-40.0%, +55.4%	2%	-26.8%, +32.8%
3.5	A	+5%	-39.7%, +56.2%	2%	-26.4%, +33.4%
	B	+5%	-39.7%, +56.1%	2%	-26.4%, +33.4%
	C	+5%	-39.7%, +56.1%	2%	-26.4%, +33.4%
	D	+5%	-40.0%, +55.3%	2%	-26.8%, +32.7%
	E	+5%	-40.1%, +55.1%	2%	-26.9%, +32.5%
4	A	+5%	-40.3%, +54.5%	2%	-27.2%, +32.0%
	B	+5%	-40.0%, +55.2%	2%	-26.8%, +32.7%
	C	+5%	-39.7%, +56.1%	2%	-26.4%, +33.4%
	D	+5%	-39.8%, +55.8%	2%	-26.6%, +33.1%
	E	+5%	-39.9%, +55.5%	2%	-26.7%, +32.8%
4.5	A	+5%	-39.9%, +55.6%	2%	-26.6%, +32.9%
	B	+5%	-39.5%, +56.6%	2%	-26.2%, +33.8%
	C	+5%	-39.9%, +55.6%	2%	-26.7%, +32.9%
	D	+5%	-40.0%, +55.2%	2%	-26.8%, +32.6%
	E	+5%	-39.7%, +56.0%	2%	-26.5%, +33.3%
5	A	+5%	-39.4%, +56.7%	2%	-26.1%, +33.9%
	B	+5%	-39.9%, +55.4%	2%	-26.7%, +32.8%
	C	+5%	-39.7%, +56.1%	2%	-26.4%, +33.4%
	D	+5%	-40.2%, +54.9%	2%	-27.0%, +32.3%
	E	+5%	-39.6%, +56.2%	2%	-26.4%, +33.4%

304
305

Figure 18. Sensitivity of deviation in friction coefficient from its optimum value on relative increase of structural acceleration for (**a**) T_{iso} =1.2 s and (**b**) T_{iso} =1.5 s and spectrum of type 2 with soil class C.

Figure 19. Sensitivity of deviation in friction coefficient from its optimum value on relative increase of structural acceleration for (**a**) T_{iso} =1.8 s and (**b**) T_{iso} =2.1 s and spectrum of type 2 with soil class C.
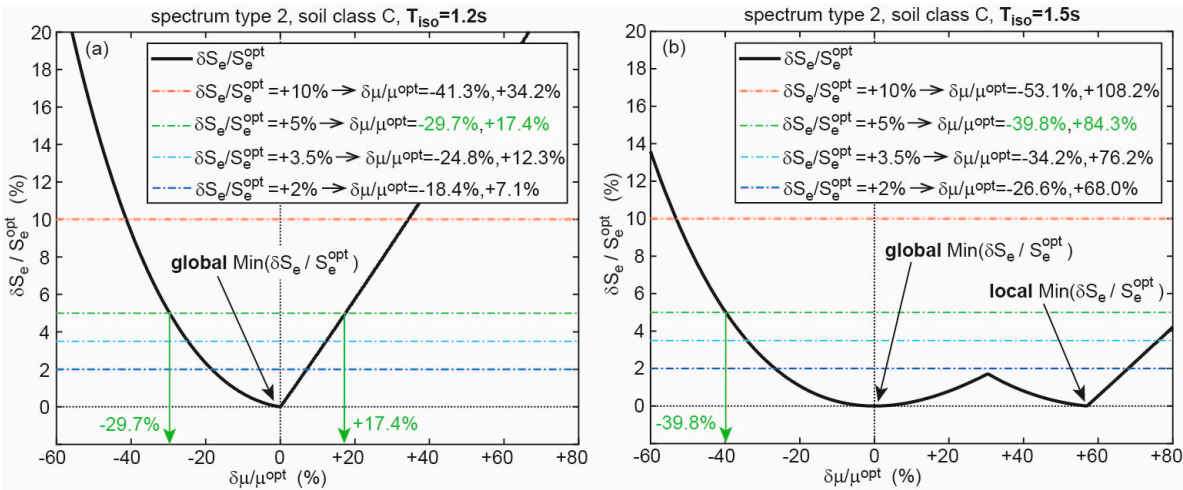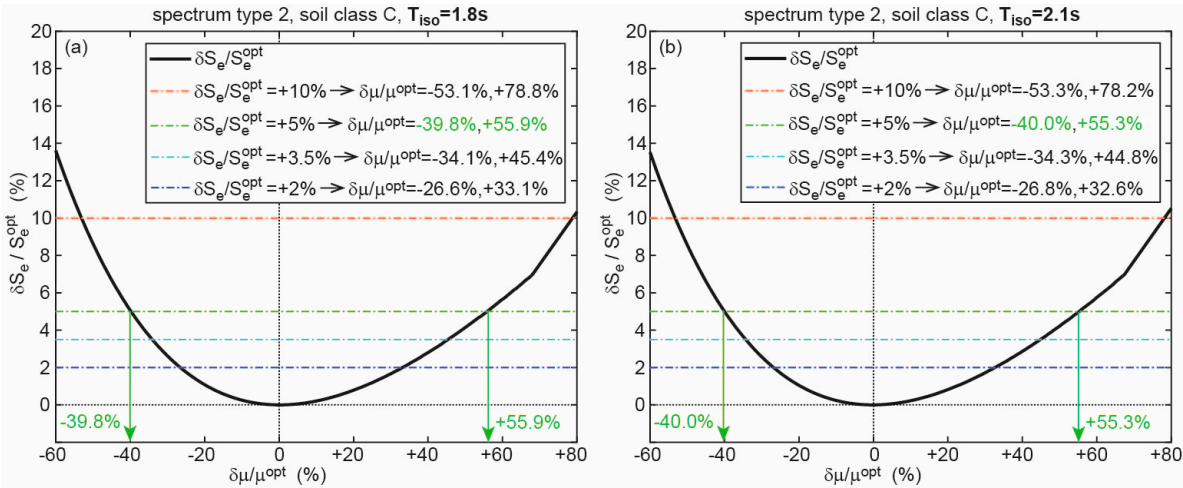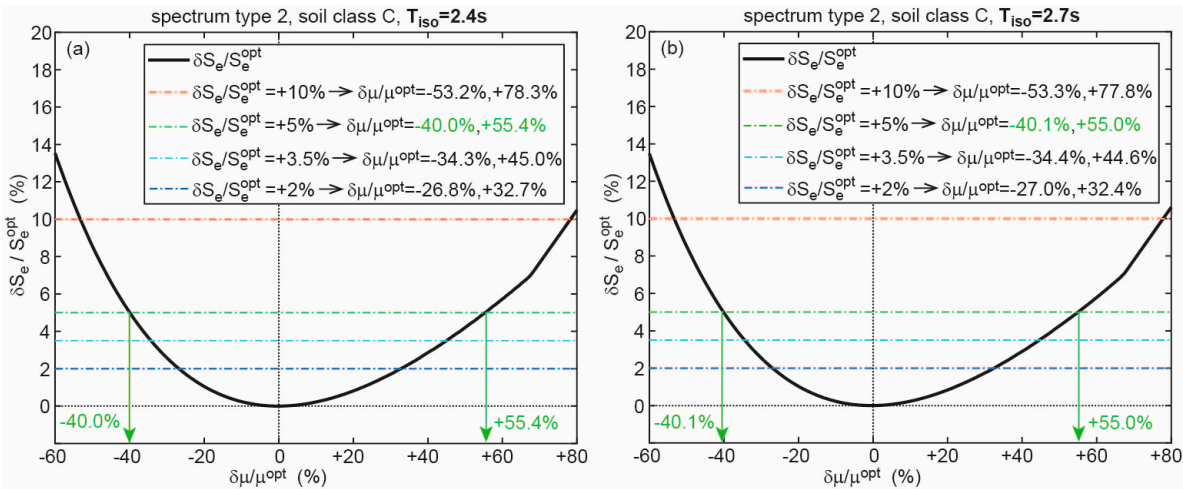

Figure 20. Sensitivity of deviation in friction coefficient from its optimum value on relative increase of structural acceleration for (**a**) T_{iso} =2.4 s and (**b**) T_{iso} =2.7 s and spectrum of type 2 with soil class C.

316   **Table 2.** Sensitivity results for spectrum of type 2 for relative increase of +5% and +2% in structural
317   acceleration.

T_{iso} (s)	soil class	$\delta S_e / S_e^{opt}$	$\delta\mu / \mu^{opt}$	$\delta S_e / S_e^{opt}$	$\delta\mu / \mu^{opt}$
1.2	A	+5%	-29.7%, +17.6%	2%	-18.3%, +7.1%
	B	+5%	-29.7%, +17.5%	2%	-18.4%, +7.1%
	C	+5%	-29.7%, +17.4%	2%	-18.4%, +7.1%
	D	+5%	-29.6%, +17.6%	2%	-18.3%, +7.2%
	E	+5%	-29.7%, +17.4%	2%	-18.4%, +7.1%
1.5	A	+5%	-39.9%, +84.1%	2%	-26.7%, +67.9%
	B	+5%	-39.8%, +84.4%	2%	-26.6%, +68.2%
	C	+5%	-39.8%, +84.3%	2%	-26.6%, +68.0%
	D	+5%	-39.9%, +84.0%	2%	-26.7%, +67.8%
	E	+5%	-39.8%, +84.3%	2%	-26.6%, +68.1%
1.8	A	+5%	-39.7%, +56.2%	2%	-26.4%, +33.5%
	B	+5%	-39.7%, +55.9%	2%	-26.5%, +33.2%
	C	+5%	-39.8%, +55.9%	2%	-26.6%, +33.1%
	D	+5%	-39.9%, +55.6%	2%	-26.6%, +33.0%
	E	+5%	-39.8%, +55.8%	2%	-26.6%, +33.1%
2.1	A	+5%	-40.0%, +55.2%	2%	-26.9%, +32.5%
	B	+5%	-40.1%, +55.0%	2%	-27.0%, +32.4%
	C	+5%	-40.0%, +55.3%	2%	-26.8%, +32.6%
	D	+5%	-40.0%, +55.3%	2%	-26.8%, +32.7%
	E	+5%	-39.7%, +56.2%	2%	-26.4%, +33.4%
2.4	A	+5%	-39.7%, +56.0%	2%	-26.5%, +33.3%
	B	+5%	-40.0%, +55.2%	2%	-26.8%, +32.6%
	C	+5%	-40.0%, +55.4%	2%	-26.8%, +32.7%
	D	+5%	-39.8%, +55.8%	2%	-26.6%, +33.1%
	E	+5%	-40.1%, +55.0%	2%	-27.0%, +32.4%
2.7	A	+5%	-39.8%, +55.7%	2%	-26.6%, +33.1%
	B	+5%	-40.1%, +54.9%	2%	-27.0%, +32.4%
	C	+5%	-40.1%, +55.0%	2%	-27.0%, +32.4%
	D	+5%	-40.0%, +55.2%	2%	-26.9%, +32.6%
	E	+5%	-39.9%, +55.6%	2%	-26.7%, +32.9%
3	A	+5%	-39.9%, +55.6%	2%	-26.6%, +32.9%
	B	+5%	-39.8%, +55.8%	2%	-26.5%, +33.2%
	C	+5%	-40.3%, +54.5%	2%	-27.2%, +32.0%
	D	+5%	-39.9%, +55.5%	2%	-26.7%, +32.8%
	E	+5%	-40.0%, +55.3%	2%	-26.8%, +32.7%

318

4. Summary and conclusions

320   This paper first presents an optimization routine that derives all valid designs of curved surface
321   sliders (CSS) based on the method of the linear response spectrum. All valid CSS designs are
322   represented by their acceleration trajectory in the elastic response spectrum plane. The fairly flat
323   minimum of the acceleration trajectory reveals that deviations in the actual friction coefficient of the
324   real CSS from its optimum value do not have great deteriorating impact on structural acceleration.
325   The second part of this study describes how friction coefficient, displacement capacity, effective
326   damping ratio, reduction factor, effective time period and re-centring condition of all optimum CSS
327   solutions for minimum structural acceleration depend on isolation time period. The results for

328 reasonable isolation time periods demonstrate that the optimum CSS, which minimizes structural
329 acceleration, is not obtained at maximum tolerated effective damping ratio of 30% of the CSS but at a
330 significantly lower value.
331   The third and final part of the paper is concerned with the question by how much the structural
332 acceleration deteriorates when the actual friction coefficient of the real CSS differs from its optimum
333 value. The underlying sensitivity analysis, which is performed for spectra of type 1 and 2 and all soil
334 classes, demonstrates that the relative increase in the structural acceleration is approximately one
335 order of magnitude smaller than the assumed deviation in the actual friction coefficient from its
336 optimum value. The sensitivity results may be used by the structural engineer to define tolerable
337 deviations in the actual friction coefficient from its optimum value such that the resulting structural
338 acceleration response is still acceptably small.

342 **Author Contributions:** Felix Weber, Leopold Meier and Johann Distl performed the optimization analysis;
343 Felix Weber and Christian Braun made the sensitivity analysis; all authors were involved in writing the paper.

344 **Conflicts of Interest:** The authors declare no conflict of interest.

References

346 1. Yen, K.Z.Y., Lee Y.J. *Passive vibration isolating system.* US Patent No. 6126136, October 3, 2000.
347 2. Eurocode 8: Design of structures for earthquake resistance – Part 1: General rules, seismic actions and
348   rules for buildings, EN 1998-1:2004 + AC:2009.
349 3. Lai, M.L., Soong, T.T. Seismic design considerations for secondary structural systems. *Journal of Structural*
350   *Engineering* (United States) **1991**; *117*, 459-472.
351 4. Inaudi, J.A., Kelly, J.M. Optimum damping in linear isolation systems. *Earthquake Engineering & Structural*
352   *Dynamics* **1993**, *22*, 583-598.
353 5. Kelly, J.M. The role of damping in seismic isolation. *Earthquake Engineering and Structural Dynamics* **1999**,
354   *28*, 3-20.
355 6. Hall, J.F., Discussion: the role of damping in seismic isolation. *Earthquake Engineering and Structural*
356   *Dynamics* **1999**, *28*, 1717-1720.
357 7. Du, Y., Zhao, G. Analysis of effect of non-classical damping on isolated structure and optimum damping.
358   *Journal of Earthquake Engineering and Engineering Vibration* **2000**, *20*, 100-107.
359 8. Jangid, R.S. Optimum friction pendulum system for near-fault motions. *Engineering Structures* **2005**, *27*,
360   349-359.
361 9. Bucher, C. Probability-based optimization of friction damping devices. *Structural Safety* **2009**, *31*, 500-507.
362 10. Kovaleva, N.V., Rutman, Yu.L., Davydova, G.V. Determination of optimal damping parameters for
363   seismic isolation systems. *Magazine of Civil Engineering* **2013**, *40*, 107-115.
364 11. Nigdeli, S.M., Bekdaş, G., Alhan, C. Optimization of seismic isolation systems via harmony search.
365   *Engineering Optimization* **2014**, *46*, 1553-1569.
366 12. Kamalzare, M., Johnson, E.A., Wojtkiewicz, S.F. Efficient optimal design of passive structural control
367   applied to isolator design. *Smart Structures and Systems* **2015**, *15*, 847-862.